



Stability Analysis of Hard Rock Pillars Under Compressive and Shear Loading Conditions Using 2D and 3D Numerical Modeling

Farzaneh Hamediazad and Navid Bahrani^(✉)

Department of Civil and Resource Engineering, Dalhousie University, Halifax, NS, Canada
navid.bahrani@dal.ca

Abstract. Numerical modeling allows for investigating the stability of mine pillars under different loading conditions. Unfavorable shear stresses may develop within mine pillars when the orebody is inclined or when the pillar axes are not aligned with in-situ principal stress directions. Quirke Mine, ON, Canada, is a typical example of a mine that experienced a chain reaction of pillar failure due to adverse shear stresses. The rib pillars at this mine were initially laid out parallel to the dip direction of an inclined orebody. In the central part of this mine, the pillars were re-oriented at 45° to the orebody dip direction. These pillars failed due to unfavorable shear loading, causing the failure of those in compression. In this study, 3D models of Quirke Mine pillars were first generated in the 3D finite element program, RS3, and their elastic stresses were compared to those of 2D models. Furthermore, the influence of pillar size and orientation relative to the in-situ principal stress directions on pillar stability was assessed using the 3D boundary element program, EX3. The outcomes of this numerical study emphasize the importance of pillar orientation and orebody dip angle in pillar design.

Keywords: Rib pillar · Pillar in shear · pillar stability · 3D numerical modeling

1 Introduction

Pillars are essential elements for the stability and integrity of underground mines. The excavation-induced damage and associated strength degradation in pillars are more significant when the orebody is inclined or when the pillar axes are not aligned with the in-situ principal stress directions. Such conditions subject the pillars to shear stresses. A pillar under such loading conditions is called a ‘pillar in shear’ [1].

The design of mine pillars is carried out using analytical, empirical and numerical methods. Although several empirical formulas and design charts have been developed for hard rock pillars (e.g., [2]), none has considered the impact of shear loading on pillar strength. Several researchers have investigated the stability of pillars in shear through analytical (e.g., [3]) and numerical (e.g., [4]) methods. Numerical modeling of pillars is usually conducted using 2D continuum and discontinuum methods. The simulation results have demonstrated the capability of 2D models in estimating the pillar strength.

However, the plane strain condition in 2D models may not always satisfy the true stress state, even for rib pillars. In this case, 3D modelling is necessary, especially for pillars under shear loading.

The central objective of this paper is to assess the stability of hard rock rib pillars of various sizes under compressive and shear loading conditions. In this regard, commercial 3D continuum numerical programs developed by Rocscience were utilized for stress and stability analyses. The case of pillar failures at the Quirke Mine, ON, Canada, has been used as a basis for this numerical study.

2 Background

2.1 Quirke Mine Pillar Failure

Quirke Mine, ON, Canada, is a classic example of a mine that experienced a chain reaction of pillar failure due to adverse shear stresses [5]. This mine consisted of 76 m-long rib pillars with a typical width-to-height (W/H) of 0.75. As shown in Fig. 1a, the pillars were initially laid out with their long axes parallel to the dip direction of the orebody with a dip angle of 20° . In a small trial area in the central part of the mine, the pillars were re-oriented at about 45° to the orebody dip direction. This realignment resulted in adverse shear stresses, progressive rock deterioration, and pillar failure. The analysis of pillar failures at the Quirke Mine is not trivial, not only due to the orebody inclination but also the orientation of pillar axes, which are not aligned with any of the in-situ principal stresses.

Figure 1b illustrates the simplified 3D geometry of this mine. Three scenarios can be assumed for the pillars at this mine: pillar long axis is (1) parallel (Case 1; Fig. 1c); (2) perpendicular (Case 2; Fig. 1d); and (3) aligned at 45° (Case 3; Fig. 1e) to the orebody dip direction. Case 1 and Case 3 correspond to the actual geometries of the pillars at the Quirke Mine. The re-orientated pillar (Case 3) has an apparent dip angle of 14° . Case 2 is the simplified geometry of the re-oriented pillars commonly used for 2D and, in some cases, 3D analyses.

Previous 2D stress analyses conducted on the Quirke Mine pillars have indicated that the re-oriented pillars were weaker than those parallel to the orebody dip direction due to the loss of confinement [4, 6]. However, in these investigations, the mutual impact of mining-induced stress changes and tensile stresses generated within the pillars due to heterogeneities were not considered in the stability analysis of these pillars. To overcome this limitation, Hamediazad and Bahrani [7] developed a 2D continuum-based heterogeneous model to simulate Quirke Mine pillar failures, which is briefly reviewed in the following section.

2.2 2D Stability Analysis of Quirke Mine Pillars Using RS2

In the numerical investigations by Hamediazad and Bahrani [7], the pillar stability analyses were carried out using the 2D finite element program, RS2 (by Rocscience). As shown in Fig. 2a, their model consists of homogeneous and heterogeneous domains. The host rock is simulated as a homogenous elastic material, while the pillar is a heterogeneous

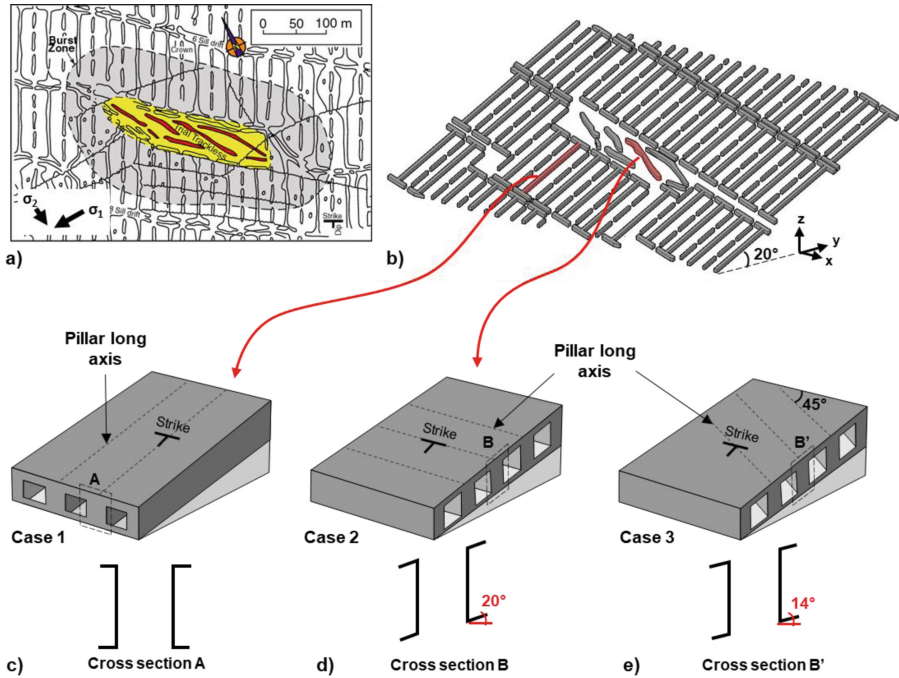


Fig. 1. (a) Plan view of Quirke Mine; (b) Quirke Mine simplified 3D geometry; and schematic of pillars with long axes: (c) parallel (Case 1); (d) perpendicular (Case 2); and (e) at 45° (Case 3) to the orebody dip direction

inelastic material consisting of several Voronoi blocks separated by joint elements. This continuum-based heterogeneous model is referred to as a Voronoi Tessellated Model (VTM) and has been used to simulate brittle rock failure at different scales [7–10]. The geometries of the modelled pillars in compression and shear are shown in Fig. 2b and Fig. 2c, respectively.

Hamediazad and Bahrani [7] conducted a series of elastic and inelastic analyses on both pillars during drift development and stope excavation. The results indicated that the pillar in shear experiences higher tensile stresses and is more prone to instability. As shown in Fig. 2d, in the pillar in compression, the failure is progressive and occurs in a relatively symmetrical manner. In the pillar in shear, the failure initiates from the opposite pillar corners and propagates diagonally to the core which is consistent with the in situ observations of pillar failure at the Elliot Lake district described by [12] (Fig. 2e).

The simulated failure mechanisms in Fig. 2 indicate that the 2D continuum-based VTM captures the overall pillar behaviour under different loading conditions. However, pillars are 3D structures, and the excavation of adjacent stopes can lead to complex stress changes within them, which may result in their failure. Therefore, a better understanding of the true stress distribution within the pillars requires 3D numerical simulations, which is the focus of the investigation in this paper.

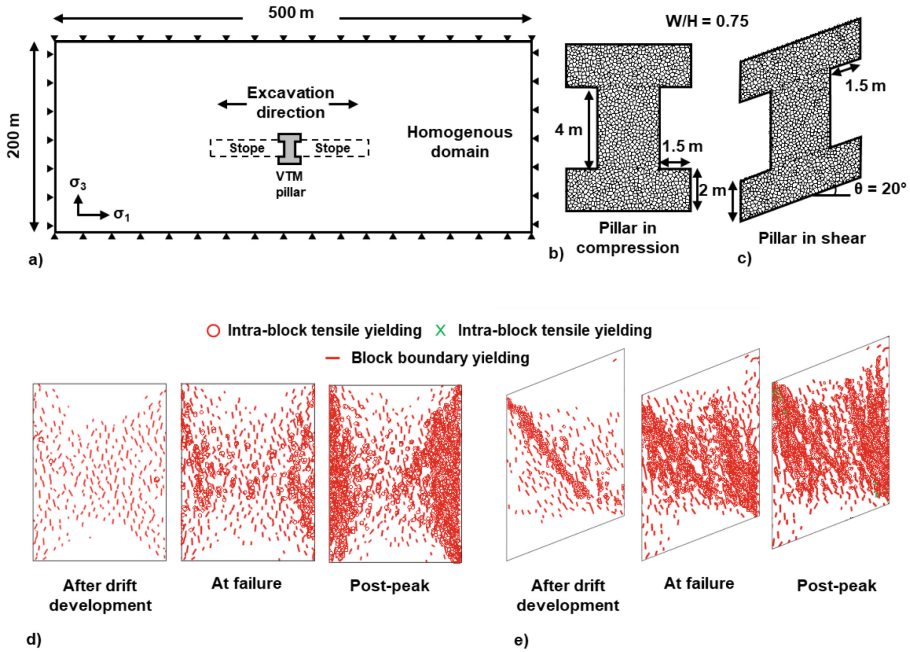


Fig. 2. (a) Geometry and boundary conditions of RS2 model. Geometry of pillars: (b) in compression; and (c) in shear. Progressive failure of pillars: (d) in compression; and (e) in shear

2.3 3D Stress Analysis of Pillars Using RS3

The 3D geometries shown in Fig. 1c and Fig. 1e were used to generate 3D pillar models in the finite element program, RS3. Figure 3 shows the RS3 model geometries for a pillar parallel to the orebody dip direction (Case 1) and that re-oriented in the trackless area (Case 3). A series of 3D stress analyses were conducted with the rock mass elastic properties used by Hamediazad and Bahrani [7] ($E = 60 \text{ GPa}$, $\nu = 0.2$). In these analyses, the in-situ stress state was consistent with that reported by Hedley et al. [11] ($\sigma_1 = 28$, $\sigma_2 = 19.5$, $\sigma_3 = 13.5 \text{ MPa}$). Note that σ_1 is horizontal and oriented at 64° to the orebody dip direction.

Figure 4 depicts the vertical stress contours within the pillars in cases 1 and 3 in the 2D and 3D models. As shown in Fig. 4a, the stress distribution in the RS3 model is comparable to that of the RS2 model. However, the results in Fig. 4b indicate that for Case 3, the 2D model exhibits a higher stress concentration near the pillar corners than the 3D model. This is attributed to the pillar geometry, which has a higher inclination angle in the 2D model than in the 3D model. The in-situ stress orientation in the RS2 model also results in a higher shear stress than that in the 3D model. Therefore, the RS2 pillar model must be used to represent the 3D pillar geometry shown in Case 2, not Case 3.

The Hoek-Brown brittle parameters ($m = 0$, $s = 0.11$) was used to determine the Extraction Ratio ($ER = \text{excavated rock volume} / \text{total volume of pillar and stope}$) at which the Factor of Safety (FoS; calculated as the ratio between strength and induced

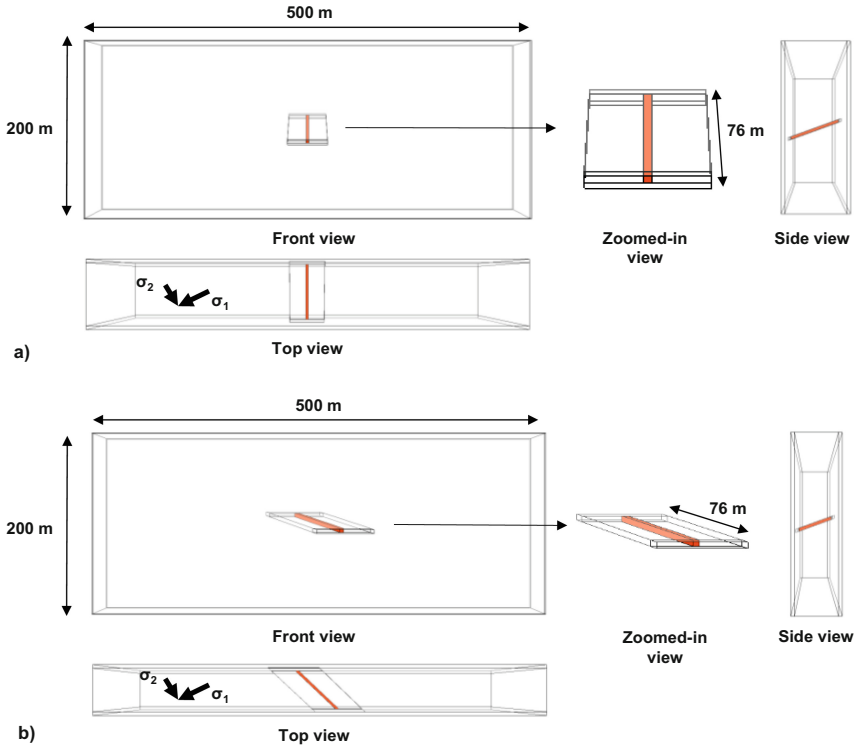


Fig. 3. 3D models of pillars at Quirke Mine constructed in RS3: (a) Case 1; and (b) Case 3

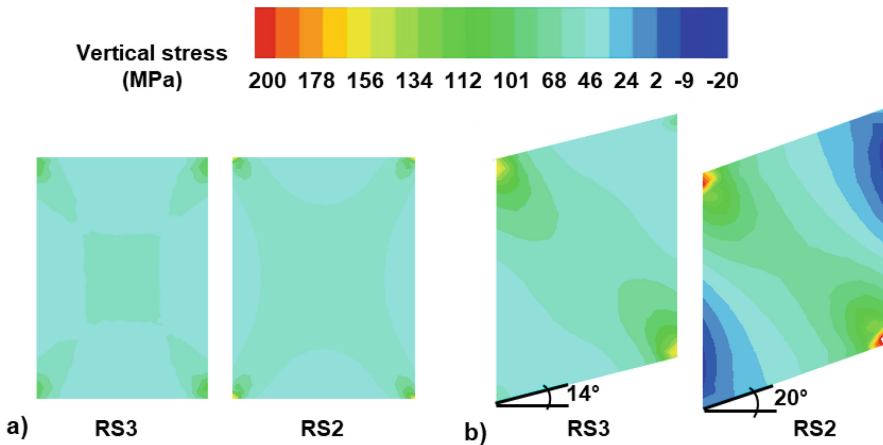


Fig. 4. Vertical stress contours in: (a) Case 1; and (b) Case 3

stress) at the pillar core becomes 1 in the pillar parallel to the orebody dip direction (Case 1 in Fig. 1). The calculated ER (88%) for Case 1 was used to analyze the induced

stresses within the pillars in Case 3. The induced stresses and FoS were then monitored along the pillar axes following stope excavations. Figure 5a and Fig. 5b show the FoS contours within the vertical sections along the short and long axes of the modeled pillars. As shown in Fig. 5a, for the same orebody geometry and in-situ stress state, the FoS at the core of the pillar in Case 1 is 1, whereas the core FoS for the pillar in Case 3 is below 1. As illustrated in Fig. 5b, the region with $FoS < 1$ at the core is extended along the long axis of the pillar in Case 3, whereas in Case 1, the core has $FoS \geq 1$ along its long axis for the entire pillar length.

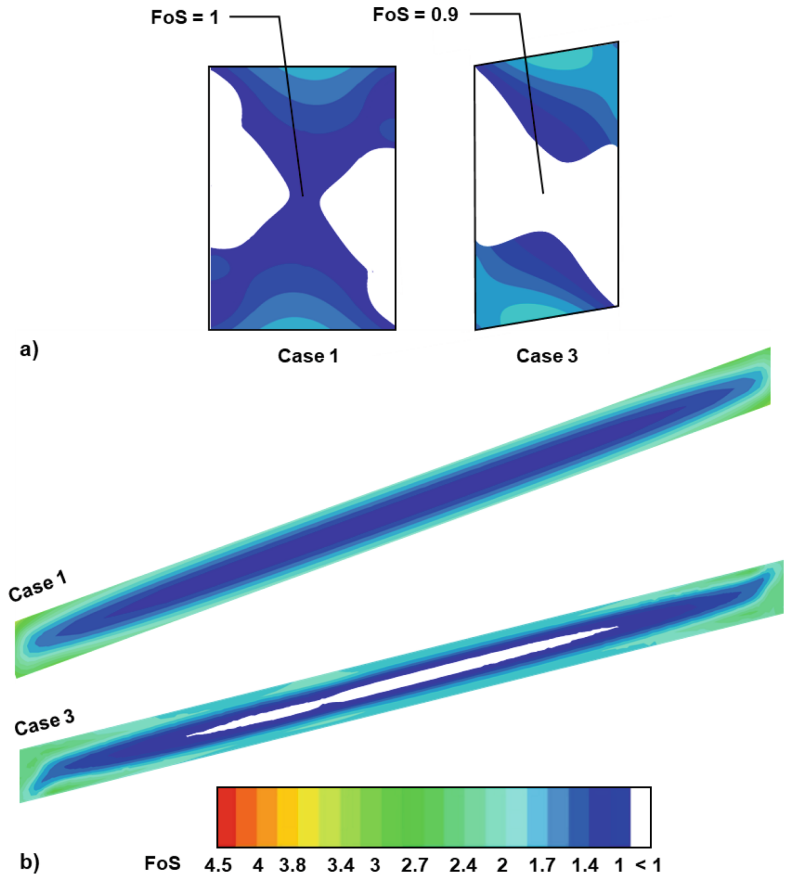


Fig. 5. Contours of FoS within vertical sections along: (a) short; and (b) long axes of the pillars in cases 1 and 3

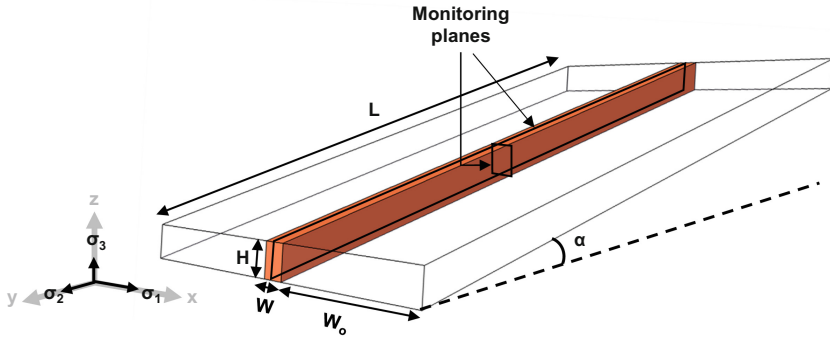


Fig. 6. 3D Geometry of a rib pillar in an inclined orebody constructed in EX3

3 3D Stress and Stability Analyses of Pillars in Shear Using EX3

3.1 Model Geometry

A series of sensitivity analyses were conducted in EX3 to investigate the influence of pillar W/H and orientation on pillar stability. Figure 6 illustrates the 3D model of a rib pillar constructed in EX3. In this figure, W , H and L are the pillar width, height and length, respectively, and α and W_o are the orebody true dip angle and the excavation (stope) width, respectively. In these analyses, H , L and W_o/W were kept constant (4 m, 76 m, and 7). To simplify the analyses, σ_1 was assumed to be parallel to the orebody strike, and σ_3 was vertical. Note that the orientations of the principal stresses in these models are not consistent with those at the Quirke Mine. Figure 6 also shows the monitoring planes in the middle of the modeled pillar along its long and short axes.

3.2 Stability Analysis

Initial stability analysis was conducted for different pillar W/H using the geometry shown in Fig. 6 for a flat orebody (i.e., $\alpha = 0^\circ$). Figure 7 illustrates the average FoS within the monitoring planes as a function of W/H for $L = 76$. As expected, the FoS increases within both monitoring planes as W/H increases. This is due to the confinement increase at the pillar core as W/H increases. Figure 7 also shows that the FoS within the vertical section along the pillar long axis is higher than that along the short axis.

To investigate the effect of shear loading on pillar stability, similar stress analyses were conducted for different pillar orientations within an inclined orebody (i.e., cases 1, 2, and 3 in Fig. 1). The induced stresses were then monitored following the stope excavation at two sides of the pillar with $ER = 88\%$. Figure 8 shows the FoS contours along the monitoring planes for the modelled pillars. As shown in this figure, the horizontal pillar and that in Case 2 have the highest and lowest FoS at their cores, respectively. As illustrated in Fig. 8b, the FoS in Case 1 is greater than 1 along its long axis. In Case 3, however, the FoS at the pillar core is lower than 1 in some areas along the long axis of the pillar.

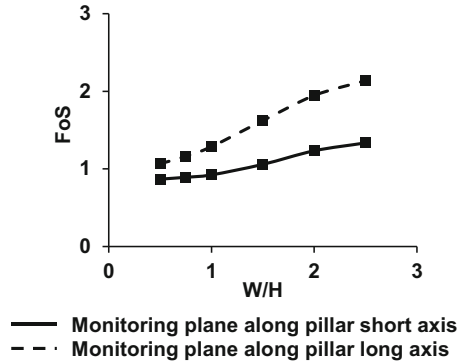


Fig. 7. Influence of W/H on average FoS in the modeled pillars in a flat orebody ($\alpha = 0^\circ$)

Further stress analyses were carried out for cases 1 and 2 with different orebody dip angles (α). The FoS at the pillar core versus α is plotted in Fig. 9a for both cases. This figure shows a reduction in FoS as α increases. As can be seen, the FoS reduction in Case 1 is subtle, whereas in Case 2, the FoS decreases more rapidly as α increases from 10° to 30° . Figure 9b and Fig. 9c depict the FoS contours within the monitoring plane along the short axes of the pillars in cases 1 and 2 for different values of α . As shown in this figure, in Case 1, as α increases from 0° to 30° , the region with $\text{FoS} < 1$ near the pillar walls gets larger and extends to the pillar core. However, in Case 2, the region with $\text{FoS} < 1$ is concentrated near the opposite pillar corners for $\alpha = 10^\circ$ and extends to the core for $\alpha = 20^\circ$ and 30° (Fig. 9c).

4 Summary and Conclusions

In this paper, RS3 was used to analyze the 3D stress distribution and factor of safety for different pillar geometries at the Quirke Mine, ON, Canada. The simulation results were compared with RS2 models. Next, the influence of the pillar size and orientation on the pillar stability was investigated through a series of sensitivity analyses in EX3.

The 3D stress analysis in RS3 showed the impact of the re-orientation of the pillars at the Quirke Mine on their stability. The pillars in the central part of this mine became unstable due to shear loading, whereas those parallel to the orebody dip direction were initially stable. The 2D and 3D stress analyses indicated that the corners of the re-oriented pillars experience higher stress concentrations in the RS2 model than the RS3 model, making the 2D stability analysis more conservative for pillars in shear.

The sensitivity analyses in EX3 indicated that increasing the pillar width increases the FoS due to the confinement increase at the pillar core. It was also found that pillar stability also depends on the orebody dip angle (α) and the orientation of their long axis relative to the principal stress directions. As α increases from 0° to 30° , the FoS decreases, and therefore, the pillars become more prone to instability. The instability potential is higher when the long axis of the pillar is perpendicular to the orebody dip direction compared to the scenario in which it is parallel to the orebody dip direction.

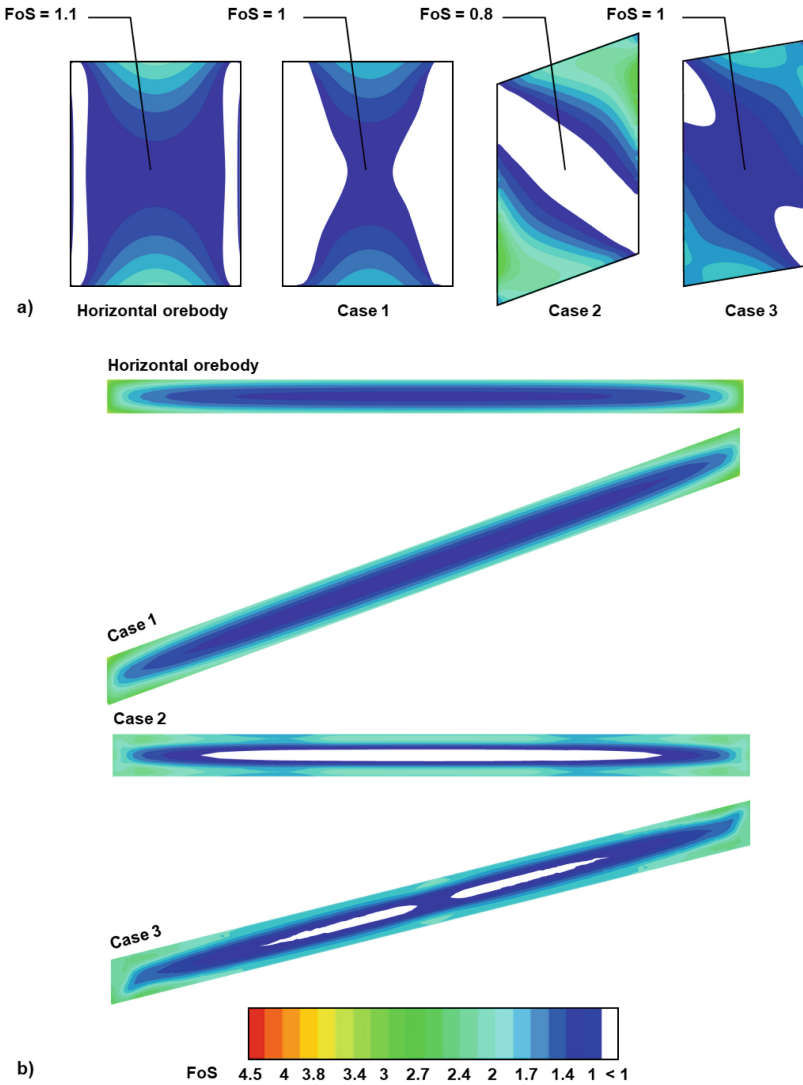


Fig. 8. Contours of FoS within monitoring planes along: (a) short; and (b) long axes for the horizontal pillar and pillars in cases 1, 2, and 3

The results of 3D numerical simulations presented in this paper emphasize the importance of pillar orientation and orebody dip angle considerations in pillar design. These factors are not considered in empirical and semi-empirical pillar design charts developed based on the pillar stability database.

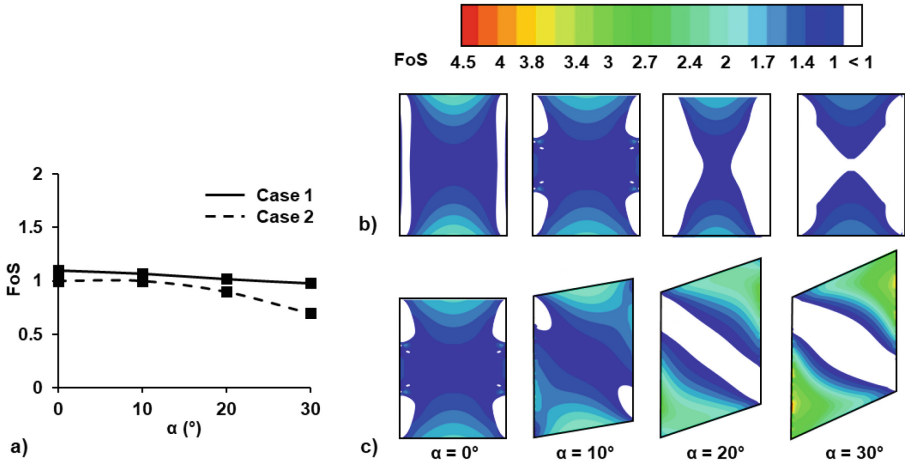


Fig. 9. (a) Influence of α on pillar core FoS. FoS contours within monitoring planes along pillar short axis in: (b) Case 1; and (c) Case 2, for different values of α

Acknowledgment. This research was supported by the Natural Sciences and Engineering Research Council of Canada (NSERC), Dalhousie University, and Rooscience through the Educational Licensing Agreement program.

References

1. Suorineni, F.T., Kaiser, P.K., Mgumbwa, J.J., Thibodeau, D.: Mining of orebodies under shear loading Part 1 – case histories. *Mining Technology*. 120: 137-147 (2011).
2. Lunder, P.J., Pakalnis, R.: Determination of the strength of hard-rock mine pillars. *Bulletin of Canadian Institute of Mining and Metallurgy*. 90: 51-55 (1997).
3. Pariseau, W.G.: Shear stability of mine pillars in dipping seams. 23rd US Symposium on Rock Mechanics (USRMS). OnePetro. (1982).
4. Suorineni, F.T., Mgumbwa, J.J., Kaiser, P.K., Thibodeau, D.: Mining of orebodies under shear loading Part 2 – failure modes and mechanisms. *Mining Technology*. 123: 240-249 (2014).
5. Hedley, D.G.F.: Rockburst Handbook for Ontario Hardrock Mines. CANMET Report SP92-1E (1992).
6. Kaiser, P.K., Diederichs, M.S., Martin, C.D., Sharp, J., Steiner, W.: Underground works in hard rock tunnelling and mining. In *ISRM international symposium*. International Society for Rock Mechanics and Rock Engineering. (2000).
7. Hamediazad, F., Bahrani, N.: Simulation of hard rock pillar failure using 2D continuum-based Voronoi Tessellated models: the case of Quirke Mine, Canada. *Computers and Geotechnics*. 148:104808 (2022).
8. Li, Y., Bahrani, N.: A continuum grain-based model for intact and granulated Wombeyan marble. *Computers and Geotechnics*. 129: 103872 (2021a).
9. Li, Y., Bahrani, N.: Strength and failure mechanism of highly interlocked jointed pillars: Insights from upscaled continuum grain-based models of a jointed rock mass analogue. *Computers and Geotechnics*. 137: 104278 (2021b).

10. Sanipour, S., Bahrani, N., Corkum, A.: Simulation of Brittle Failure Around Canada's Mine-By Experiment Tunnel Using 2D Continuum-Based Voronoi Tessellated Models. *Rock Mechanics and Rock Engineering*. 55: 6387-6408 (2022).
11. Hedley, D.G.F., Muppalaneni, S.N., Roxburgh, J.W.: A case history of rockbursts at Elliot Lake. In *Proceedings of 2nd International Conference on Stability in Underground Mining*. Lexington. New York: The American Institute of Mining, Metallurgical and Petroleum Engineers. (1984).
12. Pritchard, C.J., Hedley, D.G.F.: Progressive pillar failure and rockbursting at Denison Mine. In *Proceedings of 3rd International Symposium on Rockbursts and Seismicity in Mines*. Kingston. Rotterdam: AA Balkema (1993).

Open Access This chapter is licensed under the terms of the Creative Commons Attribution-NonCommercial 4.0 International License (<http://creativecommons.org/licenses/by-nc/4.0/>), which permits any noncommercial use, sharing, adaptation, distribution and reproduction in any medium or format, as long as you give appropriate credit to the original author(s) and the source, provide a link to the Creative Commons license and indicate if changes were made.

The images or other third party material in this chapter are included in the chapter's Creative Commons license, unless indicated otherwise in a credit line to the material. If material is not included in the chapter's Creative Commons license and your intended use is not permitted by statutory regulation or exceeds the permitted use, you will need to obtain permission directly from the copyright holder.

